Research Article

iMedPub Journals
www.imedpub.com

Archives of Medicine
ISSN 1989-5216

2020
Vol.12 No.6:32

DOI: 10.36648/1989-5216.12.6.333

Role of Ultra-Low Dose Chest CT and Chest Radiography for the Management of Coronavirus Disease 2019 (COVID-19) in the Emergency Setting

Argentieri Gianluca[1]*, Bellesi Luca[2], Pagnamenta Alberto[3], Gianluca Vanini[4], Presilla Stefano[2], Del Grande Filippo[1] and Gianella Pietro[5]

1 IIMSI - Department of Radiology, Regional Hospital, Lugano, Switzerland
2 IIMSI - Department of Medical Physics, Cantonal Hospital, San Giovanni Hospital, Bellinzona, Switzerland
3 Department of Intensive Medicine, Cantonal Hospital, Beata Vergine Hospital, Mendrisio, Switzerland
4 Department of Internal Medicine and Allergology, Cantonal Hospital, Italian Hospital, Lugano, Switzerland
5 Department of Internal Medicine and Pneumology, Cantonal Hospital, Italian Hospital, Lugano, Switzerland

***Corresponding author:**
Argentieri Gianluca

gianluca.argentieri@eoc.ch; argeg80@gmail.com

Tel: ++410918116215

Fax: ++41- (0)91 811 60 90;

Department of Radiology, Regional Hospital, Via Tesserete 46, 6900 Lugano, Switzerland.

Citation: Gianluca A, Luca B, Alberto P, Vanini G, Stefano P, et al. (2020) Role of Ultra-Low Dose Chest CT and Chest Radiography for the Management of Coronavirus Disease 2019 (COVID-19) in the Emergency Setting. Arch Med Vol.12 No.6:32

Abstract

Objectives: To determine the role of ultra-low dose chest CT compared to chest radiographs in patients with laboratory-confirmed SARS-CoV-2.

Methods: Chest radiographs and uldCT of 12 consecutive patients performed up to 48 hours from hospital admission were reviewed by 2 radiologists. Dosimetry and descriptive statistics of both modalities were analyzed.

Results and Discussion: On uldCT, parenchymal abnormalities compatible with SARS-CoV-2 pneumonia were detected in 10/12 (83%) patients whereas on chest x-ray in 8/12 (66%) and 5/12 (41%) for reader 1 and 2.

The average increment of diagnostic performance of uldCT was 29% higher than chest x-ray. The average effective dose was respectively of 0.219 and 0.073 mSv.

Conclusion: UldCT detects a substantially larger burden of inflammatory changes in symptomatic patients with suspected SARS-CoV-2 pneumonia compared to chest radiographs at the cost of a slightly higher equivalent radiation dose. It could be used as the first imaging method in an emergency department.

Keywords: Chest CT; Computed tomography; COVID-19; Dose optimization

Received: September 08, 2020; **Accepted:** October 06, 2020; **Published:** October 13, 2020

Introduction

The novel coronavirus-2 (SARS-CoV-2) infection with associated severe acute respiratory syndrome originated in China in December 2019 and reached the Lombardy region of northern Italy two months later [1,2]. Ticino is the Swiss canton neighboring Lombardy in which the first Swiss cases were diagnosed on February 25th, 2020 [3]. On the 11th of March 2020, the World Health Organization (WHO) declared SARS-CoV-2 a pandemic. At the time of the writing of this article infection due to SARS-CoV-2 continue to increase worldwide [4]. The most frequent symptoms of pneumonia caused by SARS-CoV-2 are fever and cough. Approximately 5% of infected patients are admitted to intensive care units [5]. Significant increases in C-Reactive Protein (CRP) and Lactic Acid Dehydrogenase (LDH) as well as lymphocytopenia are present in most patients with SARS-CoV-2 and are considered negative prognostic indicators [6,7]. Moreover, an increase of these biological parameters seems to correlate with the extension of infiltrates seen on chest CT scans [8].

The viral nucleic acid test, Reverse Transcription Polymerase Chain Reaction (RT-PCR) assay, has played a pivotal role in the diagnosis of SARS-CoV-2 and in clinical decision making regarding

hospitalization and isolation of individual patients, however its lack of sensitivity, insufficient stability, and relatively long processing time have proven this test to be insufficient for timely characterization in the acute clinical setting and for the progression of the pandemic [9]. The front-line radiological examination performed in these patients is usually a conventional chest radiograph, yet this modality has proven to be of limited value due to frequent false negative results [10].

By comparison, chest CT has proven to be more sensitive, with well documented features in patients with SARS-CoV-2 pneumonia [11], such as sub-pleural (peripheral), multifocal, bilateral ground glass opacities being commonly observed in more than half of patients [12,13]. In the second phase of the disease, characteristic CT signs of lung damage such as crazy-paving pattern or consolidations may appear [14]. Several studies have demonstrated the evolution of chest CT findings of SARS-CoV-2 pneumonia by classifying its radiological characteristics at different stages of infection [15-17]. Specifically, in a retrospective study, chest CTs of 121 symptomatic patients infected with SARS-CoV-2 were reviewed and during the first two days of SARS-CoV-2 infection chest CT scans showed no infiltrates in half of the patients. Subsequently (between days 6-12), infiltrates appear in >90% of cases [17]. Chest CT demonstrates a low false negative rate in the diagnosis of SARS-CoV-2 pneumonia [18] and demonstrates the effectiveness of anti-inflammatory (inhaled interferon) or non-specific antiviral (lopinavir) therapies used in a later phase of the disease [19-21]. Therefore, CT is a useful tool for diagnosis, management and therapeutic follow up of SARS-CoV-2 pulmonary infections.

Nevertheless, medical radiation exposure remains an ever-important issue due to the broad range of the patient population effected by the pandemic, which includes all ages, as well as young individuals [22]. New technologies and protocols such as ultra-low dose CT (uldCT) identify individual cases not seen on conventional radiography and can be implemented as a means of large-scale public health surveillance with reduced radiation exposures [23-25]. Therefore, in epicenters of the pandemic, uldCT could be used as a screening tool or as an adjunct to RT-PCR to exclude occult infection, especially prior to surgery or intensive immunosuppressive therapies.

The purpose of this study was to evaluate the utility of chest uldCT from initial diagnosis in the Emergency setting, compared to that of conventional chest radiographs in patients suspected for pneumonia with laboratory-confirmed SARS-CoV-2.

Materials and Methods

We reviewed 12 consecutive cases of patients with suspected SARS-CoV-2 pneumonia admitted at our institution from March 2, 2020 through March 12, 2020. A suspected SARS-CoV-2 case was defined as a patient presenting fever (≥ 38°C) or respiratory symptoms (cough, dyspnea). Clinical samples for SARS-CoV-2 diagnostic testing were obtained in accordance with WHO guidelines. Nasopharyngeal and oropharyngeal swab specimens were collected with synthetic fiber swabs and the swabs were inserted into the same sterile tube containing 2 to 3 mL of viral transport medium. Influenza, Pneumococcus and Legionella tests excluded other possible intercurrent infections. In 1 case virus identification was carried out with bronchoalveolar lavage (BAL) and specimens were extracted and subjected to next-generation sequencing. All patients (12/12) resulted SARS-CoV-2 positive with these laboratory tests, which we considered the reference standard for the purposes of our study.

Chest X-Ray and CT protocol

In order to identify any signs of pneumonia at admission in the emergency room, all patients suspected of SARS-CoV-2 underwent baseline digital anterior-posterior chest radiography at full inspiration using a mobile chest radiograph device (Philips Mobile Diagnost wDR, Philips Medical System SA).

We performed chest uldCT in patients with signs of respiratory failure (FIO_2/PaO_2 <300 mmHg), with clinical SARS-CoV-2 compatible symptoms or with suspicious SARS-CoV-2 parenchymal changes at chest x-ray. Chest uldCT images were obtained at 22.5 ± 14.1 hours (range, 3-48 hours) from chest x-ray acquisition using two multi-detector scanners: Siemens Somatom Definition Flash and Siemens Somatom Definition Edge (Siemens, Erlangen, Germany). Scan parameters were optimized for a patient with a normal BMI between 18.5 and 24.9 as follows: tube voltage 80 kVp; fix tube current of 20 mAs without automatic exposure control; slice thickness 2.0 mm; reconstruction interval 2 mm; with a sharp reconstruction kernel. CT images were acquired with the patient in the supine position at full inspiration, without intravenous contrast medium.

Image analyses

Two radiologists with different specialty skills: thoracic, reader 1 (R1) and general, reader 2 (R2), with respectively 10 and 17 years of experience (G.A. and F.DG.), reviewed both chest radiographs and CT images on two different days in order to reduce the recall bias. On the first day the readers reviewed the chest radiographs and on the second day the CT scans, both series randomly presented. The CT images were evaluated with both lung (width, 1500 HU; level, -600 HU) and mediastinal (width, 400 HU; level, 40 HU) window settings.

Images were reviewed on a professional picture archiving and communication system (PACS) PC workstation (Philips Intellispace PACS). For the purpose of our study a peripheral location was defined as the outer third of the lung parenchyma. The readers assessed both chest radiographs and uldCT only for the presence of parenchymal abnormalities compatible with SARS-CoV-2 infections. The number of lobes involved (from 0 to 5 lobes), the location (central, peripheral or both) and opacity density (ground-glass, consolidation or both) based on the Fleischner Society glossary of terms for thoracic imaging were annotated. Mediastinal and osseous structures were not evaluated.

Dose analysis

CT effective dose and equivalent organ dose calculation were obtained with Radiometric (Bayer Medical Care Inc., Indianola, PA, USA), a web-based software platform, using an available Monte Carlo interactive dosimetry tool essentially superimposing real CT images with virtual Christy phantoms available inside the

software. The software automatically matched the phantom and the patient scanogram and calculated the organ specific radiation doses as well as the global radiation parameter, expressed in mSv, according to the tissue weighting factors reported in ICRP103 and in ICRP 60 [26]. Dose Area Product (DAP) and patient data related to each radiographic exam were transferred into Radiometric. After data collection, the PC-based Monte Carlo program for x-ray simulation, PCXMC (STUK, Helsinki, Finland), was used to calculate effective dose, organ doses and assessment of exposure for radiographic exams [27].

Statistical analysis

For descriptive statistics, categorical variables were expressed as absolute numbers with percentages, normally distributed quantitative variables as mean ± Standard Deviation (SD) and non-normally distributed variables as median with an Interquartile Range (IQR). To assess the agreement between the two radiologists concerning the different radiological categorical variables, kappa statistics were presented as follows: 0 very poor; 0.01-0.20 poor; 0.21-0.40 discreet; 0.41-0.60 moderate; 0.61-0.80 good; 0.81-1.00 excellent [28]. Stata version 15 (StataCorp. LP, College Station, TX, USA) was used for all statistical analyses.

Results

Clinical findings

A total of 12 laboratories proven SARS-CoV-2 patients (mean age, 57.8 ± 13.6 years, 58% male) were included. Three patients (25%) fulfilled the criteria of mild (200 mm Hg < PaO_2/FIO_2 ≤ 300 mm Hg) Acute Respiratory Distress Syndrome (ARDS) and one (8%) the criteria of moderate (100 mm Hg < PaO_2/FIO_2 ≤ 200 mm Hg) ARDS. We observed CRP elevations in 83% of patients (mean CRP, 78 ± 76 mg/L). LDH could be assessed in 10 out of 12 patients and in nine out of ten (90%) we recorded elevated values (mean LDH, 475 ± 220 mg/L) **(Table 1).** Two out of 12 patients (16%) had positive urinary antigen for Legionella and pneumococcus and two out of 12 patients (16%) had positive swab results for Influenza A, B and Respiratory Syncytial Virus.

Inter-reader-, chest radiographic- and CT- findings, R1 reported the absence of radiographic abnormalities (ground glass, consolidation or both) in four (33%) patients and R2 reported the absence of these findings in seven patients (58%).

The inter-reader agreement for bilateral distribution was moderate (kappa value=0.5). On chest radiographs the distribution of abnormalities was described in the sub-pleural regions in six patients (50%) by R1 and in one patient (8%) by R2 (kappa value=0.5). A central location and combined central and peripheral locations were observed respectively in four patients (33%) by R1 and in zero patients (0%) by R2 (kappa value = 0.62), and in two patients (16%) by R1 and in four patients (33%) by R2 (kappa value=0.57) **(Table 2).**

By contrast, on chest uldCT both readers excluded parenchymal abnormalities (ground-glass, consolidation or both) in 16% of the cases. At CT the inter-observer agreement for bilateral distribution was perfect (kappa value=1).

The distributions of these abnormalities on uldCT were described in subpleural regions in nine patients (75%) by R1 and in ten patients (83%) by R2 (kappa value=0.75); in a predominantly central location in nine patients (75%) by R1 and in eight patients (66%) by R2 (kappa value = 0.8); and in both central and peripheral locations in eight patients (66%) by both R1 and R2 (kappa value=1) **(Table 2).** At uldCT abnormalities in 10/12 (83%) SARS-CoV-2 patients were detected by both readers with a sensitivity of 83%.

Using uldCT as a reference, pulmonary abnormalities compatible with SARS-CoV-2 pneumonia were detected when using chest x-ray in 8/12 (66%) cases by R1 and in 5/12 (41%) cases by R2.

These values corresponded with the chest x-ray sensitivity for each reader. The average sensitivity for this method was therefore 54%.

All lobes were reported to be affected on chest radiographies in respectively 0/12 (0%) by R1 and in 1/12 (8%) by R2, which differed at uldCT with 4/12 (33%) patients by R1 and 6/12 (50%) patients by R2.

The increment of diagnostic performance for R1 with uldCT was about 16% higher than chest-x-ray while for R2 was 42%, with an average value of 29% for both readers.

Given the absence of asymptomatic or negative SARS-CoV-2 patients in our population in our study, specificity, VPP and VPN were not calculated. For the same reason, accuracy for chest radiographies and uldCT corresponded with the sensitivities of both diagnostic modalities.

Dosimetry results

For chest radiography, average effective dose was 0.073 mSv with an average lung equivalent dose of 0.143 mSv and an average DAP equal to 194 mGy cm^2 **(Tables 3 and 4).**

For uldCT average effective dose was 0.219 mSv while average lung equivalent dose was 0.498 mSv with an average CTDI value equal to 0.433 mGy and average DLP value of 14.3 mGycm **(Tables**

Table 1 Patient data with inflammation and oxygenation indices.

Patient	1	2	3	4	5	6	7	8	9	10	11	12
Sex	F	M	F	M	F	M	F	M	F	M	M	M
Age	47.6	58.5	57.0	62.1	45.1	46.9	81.1	70.9	50.6	83.3	44.1	50.1
CRP, mg/L (< 5)	113	2	74	18	2	271	91	29	14	98	133	86
LDH, U/l (140-280)	479	506	534	456	270	578	466	-	-	514	906	383
FIO_2/PaO_2, mmHg (>400)	236	325	321	336	432	196	204	400	321	275	368	375

CRP: C-Reactive Protein; LDH: Lactate Dehydrogenase

Table 2 Presence and distribution of radiological findings for reader 1 and 2 for Chest radiographs and uldCT.

Variables	RX		CT	
	R1	R2	R1	R2
No. of lobes affected	100% (12/12)	100% (12/12)	100% (12/12)	100% (12/12)
0	33% (4/12)	58% (7/12)	16 % (2/12)	16 % (2/12)
1	8% (1/12)	8 % (1/12)	8 % (1/12)	8 % (1/12)
2	8% (1/12)	8% (1/12)	16 % (2/12)	16 % (2/12)
3	41% (5/12)	8% (1/12)	25 % (3/12)	8 % (1/12)
4	0% (0/12)	8% (1/12)	0 % (0/12)	0 % (0/12)
5	8% (1/12)	8% (1/12)	33 % (4/12)	50 % (6/12)
Ground-glass opacities	58% (7/12)	8 % (1/12)	75 % (9/12)	33 % (4/12)
Consolidation	41% (5/12)	33 % (4/12)	16 % (2/12)	8 % (1/12)
Ground-glass opacities and consolidation	33 % (4/12)	0 % (0/12)	8 % (1/12)	41 % (5/12)
Bilateral disease	50 % (6/12)	25 % (3/12)	75 % (9/12)	75 % (9/12)
Peripheral distribution	50 % (6/12)	8 % (1/12)	75 % (9/12)	83 % (10/12)
Central distribution	33 % (4/12)	0 % (0/12)	75 % (9/12)	66 % (8/12)
Central and peripheral distribution	16 % (2/12)	33 % (4/12)	66 % (8/12)	66 % (8/12)

Table 3 Exam data and dose estimations for radiographic exams with PCXMC.

RADIMETRICS Data					PCXMC	
Patient No	Projection	kV	Proiection	DAP (mGy cm2)	Dose to Lungs (mSv)	Effective Dose ICRP 103 (mSv)
1	Supine	100	AP	104.7	0.073	0.037
2	Standing	100	AP	162.0	0.135	0.067
3	Supine	100	AP	178.8	0.140	0.075
4	Supine	102	AP	226.2	0.173	0.089
5	Sitting	100	AP	198.0	0.153	0.079
6	Supine	100	AP	120.5	0.094	0.048
7	Sitting	100	AP	108.6	0.087	0.045
8	Standing	125	AP+LAT	340.4	0.146	0.069
9	Standing	100	AP	361.3	0.284	0.149
10	Supine	117	AP	165.7	0.140	0.071
11	Supine	100	AP	157.0	0.121	0.062
12	Supine	100	AP	209.5	0.164	0.088

Table 4 Statistical data analysis for radiographic exams.

Radiography	DAP (mGy cm^2)	Dose to Lungs (mSv)	Effective Dose ICRP 103 (mSv)
Media	194.4	0.143	0.073
Median	172.3	0.140	0.070
75 percentile	213.7	0.156	0.081
St.Dev.	82.5	0.054	0.029

5 and 6). At our institution dosimetry values for a standard low-dose chest CT are as follow: CTDI: 3.3 ± 1.102 mGy; DLP: 121.1 ± 49.23 mGycm; effective dose: 2.31 ± 0.81 mSv. Data were extracted with Radiometric.

Discussion

In our study uldCT proved to be a non-invasive imaging modality with slightly higher radiation dose, but with substantially higher accuracy compared to chest radiography. The average effective dose of a chest radiography taken in just one projection was 0.073 mSv at our institution. Typical effective dose reported for chest radiography should have values lower than 0.07 mSv depending on age and specific conditions [24,29]. According to our results, the average effective dose recorded for a chest uldCT was 0.219 mSv, meaning that the average effective dose of a chest uldCT was about 3 times higher than that of a chest radiograph. In the current literature, chest uldCT is usually associated with a radiation dose varying from 0.14 to 0.5 mSv [23,24]. For this dose range no standardized reference values have been published as of yet.

In our series up to 58% of patients with SARS-CoV-2 suspected pneumonia had a negative chest x-ray. This data underpins the

Table 5 Exam data and dose estimations for CT exams with RADIMETRICS.

RADIMETRICS					
Patient No	Date of CT	CTDI (mGy)	DLP (mGy cm²)	Effective Dose ICRP 103 (mSv)	Equivalent dose to Lung (mSv)
1	43897	0.4	15	0.171	0.427
2	43893	0.4	12.8	0.289	0.615
3	43897	0.4	12.9	0.263	0.545
4	43896	0.5	17	0.279	0.657
5	43896	0.5	16.3	0.159	0.391
6	43903	0.4	15	0.188	0.455
7	43901	0.5	17.3	0.166	0.398
8	43899	0.4	9.9	0.22	0.499
9	43902	0.5	14.8	0.288	0.571
10	43897	0.4	13.9	0.207	0.528
11	43899	0.4	13.3	0.155	0.404
12	43902	0.4	13.1	0.239	0.485

Table 6 Statistical data analysis for CT exams.

CT	CTDI (mGy)	DLP (mGy cm²)	Effective Dose ICRP 103 (mSv)	Equivalent dose to Lung (mSv)
Media	0.433	14.275	0.219	0.498
Median	0.400	14.350	0.214	0.492
75 percentile	0.500	15.325	0.267	0.552
St.Dev.	0.049	2.082	0.052	0.088

limited diagnostic value of chest x-ray, due to the prevalence of false negative results [10]. In our study UldCT resulted positive for the presence of suspicious pulmonary ground-glass infiltrates or consolidations in 83% of the cases. A larger Chinese study by Ai and colleagues demonstrated 88% positive cases by utilizing low dose chest CT [30].

Our study demonstrated that at early (≤ 48h) chest uldCT ground-glass infiltrates, with or without consolidation, presented predominantly in combined locations peripheral and central (kappa value=1), with chiefly bilateral involvement (kappa value=1). These results are similar to those studies of viral pneumonia described in the literature which utilized standard chest CT [12,13,15].

On chest radiographs, most of the pulmonary alterations had ambiguous localizations. The concordance of infiltrate distribution among each lobe for both readers was poor (kappa value=0.33). Ground-glass infiltrates were difficult to evaluate (kappa value=0.13), while the concordance for consolidation was higher (kappa value=0.47). This is probably due to readers' subjective interpretations of density and radiographic transparency.

At uldCT, ground-glass infiltrates proved easier to evaluate and agreement to that of chest radiographs was superior (kappa value=0.55) although, probably due to the heterogeneity of the involvement of the lung parenchyma, agreement on infiltrate distribution among each lobe, as well as agreement on the evaluation of regions of pulmonary consolidation were poor (kappa value=0.33).

In accordance with the findings of Yoon et al., our experience shows that chest x-ray still underestimates the diagnosis of SARS-CoV-2 pneumonia even when compared to an ultra-low dose CT protocol [10]. We discovered that in cases where all lobes were involved on uldCT images (33-50% of cases), only 0-8% of chest radiographs appeared abnormal. The performance of both readers improved by approximately 29% using uldCT, when compared to that demonstrated with chest radiographies.

This improvement proved even higher (42%) for the general radiologist, suggesting that this modality could assist radiologists not sub-specialized in thoracic radiology, particularly during this critical pandemic period when there is an abundance of thoracic exams. Therapy management was also assessed in our series using uldCT.

In one case therapy involving 3 days of treatment with lopinavir/ritonavir and hydroxychloroquine followed by ten days of remdesivir demonstrated progressive healing documented by uldCT follow-up examinations on day nine and 15 **(Figures 1C-1D).** Other studies have already used standard chest CT to document therapeutic follow-up in similar cases treated with non-specific anti-viral antibodies [17], but not with a chest uldCT protocol.

In a second case, chest radiographs showed ill-defined bilateral abnormalities **(Figure 2A)** with SARS-CoV-2 nasopharyngeal and oral swabs negative on admission.

Chest uldCT showed instead typical diffuse ground glass infiltrates, highly suggestive of viral pneumonia **(Figures 2B and 2C).** The swab test was repeated and resulted again negative, whereupon a third test obtained by bronchoalveolar lavage (BAL) finally confirmed the diagnosis of SARS-CoV-2 pneumonia.

In a third and last case, a chest x-ray performed in the sitting position initially did not show clear infiltrates **(Figure 3A)** despite the clinical suspicion of SARS-CoV-2 infection, which was later confirmed by laboratory results.

Chest uldCT revealed the presence of typical sub pleural ground-

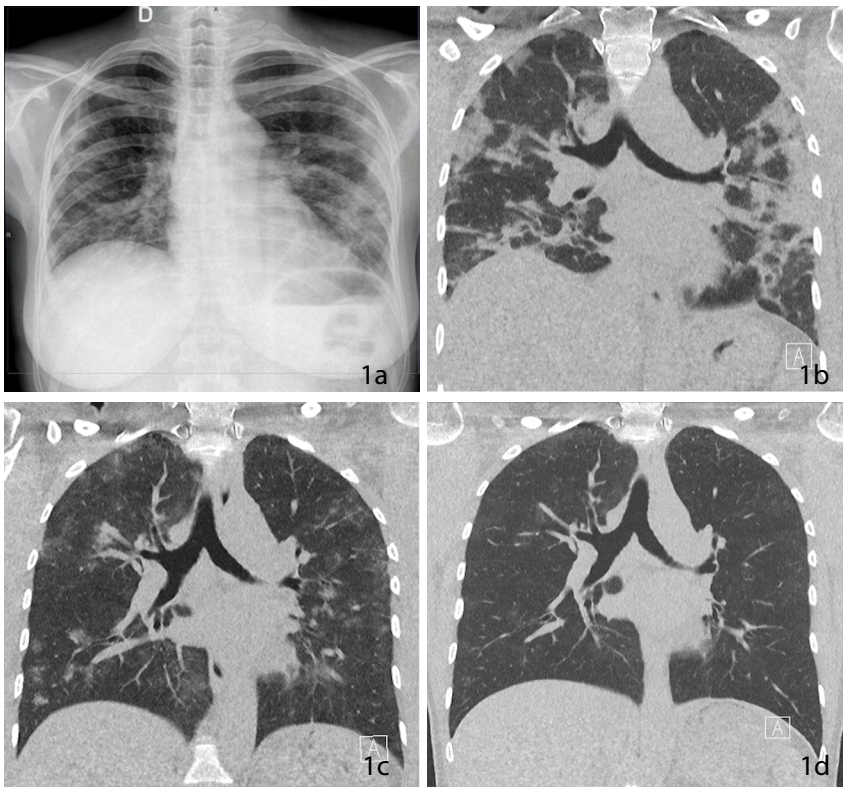

Figure 1 Progressive healing from day 1, 2, 9 and 15 of bilateral infiltrates with sub pleural distribution.

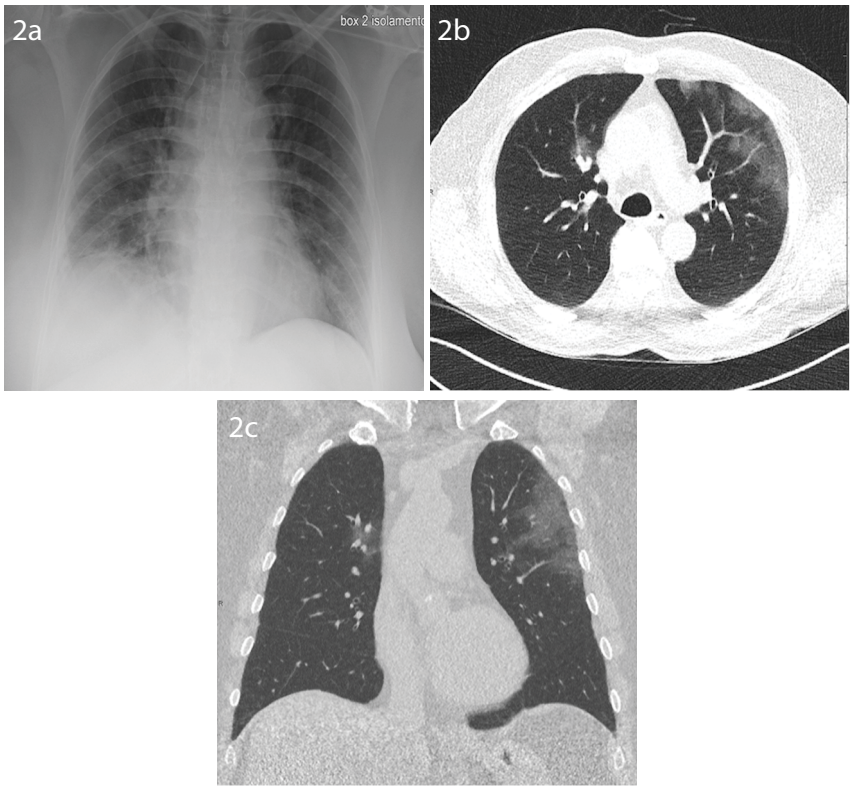

Figure 2 **(A)** Patient 3 Chest X-ray showed ill-defined infiltrates on the right mid and basal fields. **(B and C)** Diffuse bilateral infiltrates on uldCT (B and C).

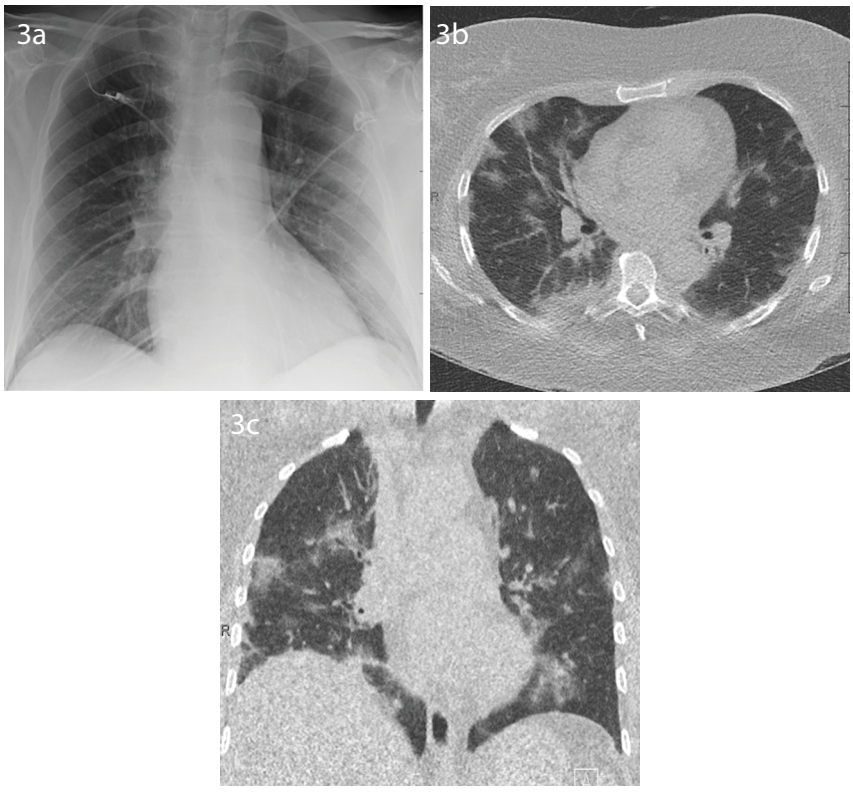

Figure 3 **(A)** Suboptimal, apparently unremarkable chest radiograph. **(B and C)** Patchy bilateral areas of ground glass on ultra-uldCT.

glass opacities in both upper lobes, highly consistent with SARS-CoV-2 viral pneumonia **(Figures 3B and 3C)**. The last two cases demonstrate the critical diagnostic value of chest uldCT.

A few limitations exist in this study. First, the number of included patients was small, because of the very early phase of this outbreak in our region (180 new registered cases up to 12th of March) [31]. Including more patients would enable a more generalizable assessment of the radiologic findings of SARS-Cov-2 pneumonia. Second, the study was retrospective and despite the median for the delay between chest x-ray and chest uldCT examinations being 22.5 hours, the range was wide (3-48 hours). This wide range, could potentially interfere with the correlation of findings between these two modalities, but suggests time that could have been saved if uldCT was the first and only modality used.

Third, the PCXMC phantoms have two potential limitations for accurate dosimetry: over-simplified stylized phantoms and anatomical structures not completely comparable to voxel or hybrid phantoms potentially lead to unrealistic, over-simplified adjustment of body size.

Conclusion

In conclusion, our results suggest that chest uldCT detects a substantially larger burden of inflammatory changes in patients with suspected SARS-CoV-2 pneumonia when compared to conventional chest radiography, at the cost of a slightly higher equivalent radiation dose. In patients admitted at emergency department with high clinical suspicion and negative RT-PCR results, implementing the ultra-low dose chest CT protocol could improve diagnostic performance during the early phase of this disease.

Disclosure

No funding was received for this work from: National Institutes of Health (NIH); Wellcome Trust; Howard Hughes Medical Institute (HHMI) or any other organization.

Conflict of Interest

The author(s) declare(s) that there is no conflict of interest.

Ethics Approval and Consent to Participate

This retrospective study was approved by our local ethics committee (2020-00568 CE 3606) and the need for patient consent was waived.

Availability of Data and Materials

Data will not be shared because of dimension and number of files involved.

Competing Interests

The authors declare that they have no competing interests.

References

1 Tian S, Hu N, Lou J, Kun Chen, Kang X, et al. (2020) Characteristics of COVID-19 infection in Beijing. J Infect 80: 401-406.

2 https://www.salute.gov.it/portale/nuovocoronavirus/dettaglioContenutiNuovoCoronav irus.jsp?lingua=italiano&id=5351&area=nuovoCoronavirus&menu=vuoto.

3 https: //www4.ti.ch/dss/dsp/COVID19/home/#c542005.

4 https: //www.who.int/dg/speeches/detail/who-director-general-s-opening-remarks-at-the-media-briefing-on-COVID-19---11-march-2020.

5 Guan WJ, Ni ZY, Hu Y (2020) Clinical Characteristics of Coronavirus Disease 2019 in China. N Engl J Med 30: 1708-1720.

6 Huang C, Wang Y, Li X (2020) Clinical features of patients infected with 2019 novel coronavirus in Wuhan, China. Lancet 395: 497-506.

7 Guan WJ, Ni ZY, Hu Y (2020) Clinical characteristics of 2019 novel coronavirus infection in China. N Engl J Med 382: 1708-1720.

8 Xiong Y (2020) Clinical and High-Resolution CT Features of the COVID-19 Infection: Comparison of the Initial and Follow-up Changes. Invest Radiol 55: 332-339.

9 Yang Y, Yang M, Shen C (2020) Evaluating the accuracy of different respiratory specimens in the laboratory diagnosis and monitoring the viral shedding of 2019-nCoV infections. medRxiv.

10 Yoon SH, Lee KH, Kim JY (2020) Chest Radiographic and CT Findings of the 2019 Novel Coronavirus Disease (COVID-19): Analysis of Nine Patients Treated in Korea. Korean J Radiol 21: 494-500.

11 Kanne JP, Little BP, Chung JH (2020) Essentials for Radiologists on COVID-19: An Update-Radiology Scientific Expert Panel. Radiology 27: 200527.

12 Zhou S, Wang Y, Zhu T (2020) CT Features of Coronavirus Disease 2019 (COVID-19) Pneumonia in 62 Patients in Wuhan, China. Radiology 4: 200230.

13 Kanne JP (2020) Chest CT Findings in 2019 Novel Coronavirus (2019-nCoV) Infections from Wuhan, China: Key Points for the Radiologist. Radiology 295: 16-17.

14 Chung M, Bernheim A, Mei X (2020) CT Imaging Features of 2019 Novel Coronavirus (2019-nCoV). Radiology 295: 202-207.

15 Shi H, Han X, Jiang N (2020) Radiological findings from 81 patients with COVID-19 pneumonia in Wuhan, China: A descriptive study. Lancet Infect Dis 20: 425-434.

16 Pan Y, Guan H, Zhou S, Wang Y, Li Q, et al. (2020) Initial CT findings and temporal changes in patients with the novel coronavirus pneumonia (2019-nCoV): a study of 63 patients in Wuhan, China. Eur Radiol 30: 3306-3309.

17 Bernheim A, Mei X, Huang M (2020) Chest CT Findings in Coronavirus Disease-19 (COVID-19): Relationship to Duration of Infection. Radiology 295: 200463.

18 Li Y, Xia L (2020) Coronavirus Disease 2019 (COVID-19): Role of Chest CT in Diagnosis and Management. AJR Am J Roentgenol 214: 1280-1286.

19 Duan YN, Qin J (2020) Pre and Posttreatment Chest CT Findings: 2019 Novel Coronavirus (2019-nCoV) Pneumonia. Radiology 295: 21.

20 Lei J, Li J, Li X, Qi X (2020) CT Imaging of the 2019 Novel Coronavirus (2019-nCoV) Pneumonia. Radiology 295: 18.

21 Wei J, Xu H, Xiong J, Shen S, Fan B, et al. (2020) 2019 Novel Coronavirus (COVID-19) Pneumonia: Serial Computed Tomography Findings. Korean J Radiol 21: 501-504.

22 Kang Z, Li X, Zhou S (2020) Recommendation of low-dose CT in the detection and management of COVID-2019. Eur Radiol 30: 4356-4357.

23 Kim Y, Kim YK, Lee BE, Ju Ryu Y, Jeong Lee S, et al. (2015) Ultra-Low-Dose CT of the Thorax Using Iterative Reconstruction: Evaluation of Image Quality and Radiation Dose Reduction. AJR Am J Roentgenol 204: 1197-202.

24 Vilar-Palop J, Vilar J, Hernández-Aguado I, González-Álvarez I, Lumbreras B (2016) Updated effective doses in radiology. J Radiol Prot 6: 975-990.

25 Kroft LJM, Van der Velden L, Girón IH, Roelofs JJH, De Roos A, et al. (2019) Added Value of Ultra-low-dose Computed Tomography, Dose Equivalent to Chest X-Ray Radiography, for Diagnosing Chest Pathology. J Thorac Imaging 4: 179-186.

26 The 2007 Recommendations for the International Commission on Radiological Protection. ICRP publication 103. Ann ICRP 37: 1-332.

27 http: //citeseerx.ist.psu.edu/viewdoc/download?doi=10.1.1.194.1691&rep=rep1&type=pdf

28 Richard LJ, Gary GK (1977) The measurement of observer agreement for categorical data. Biometrics 33: 159-174.

29 https: //clinicaltrials.gov/ct2/show/NCT03922516.

30 Ai T, Yang Z, Hou H, Zhan C, Chen C, et al. (2020) Correlation of Chest CT and RT-PCR Testing in Coronavirus Disease 2019 (COVID-19) in China: A Report of 1014 Cases. Radiology 296: E32-E40.

31 https://www.bag.admin.ch/bag/en/home/krankheiten/ausbrueche-epidemien-pandemien/aktuelle-ausbrueche-epidemien/novel-cov/situation-schweiz-und-international.html